

Electrical deactivation by vacancy-impurity complexes in highly As-doped Si

V. Ranki and K. Saarinen

Laboratory of Physics, Helsinki University of Technology, P. O. Box 1100, FIN-02015 HUT, Finland

J. Fage-Pedersen, J. Lundsgaard Hansen, and A. Nylandsted Larsen

Institute of Physics and Astronomy, University of Aarhus, DK-8000 Aarhus C, Denmark

(Received 14 August 2002; revised manuscript received 14 November 2002; published 22 January 2003)

We have applied positron annihilation and Hall-effect/resistivity experiments to identify and quantify vacancy-impurity complexes formed in molecular-beam epitaxially grown Si at very high As doping levels of $>10^{20} \text{ cm}^{-3}$. The results indicate that V-As₃ is the dominant vacancy defect which exists at concentrations relevant to the electrical deactivation of doping. Larger complexes, tentatively identified as V₂-As₅, are also present at high concentrations. The V-As₃ and V₂-As₅ defects are removed by annealings at 800 °C and 900 °C, respectively. The rapid thermal annealing leads to lowest concentrations of these deactivating defects, indicating that their formation is limited by migration processes during the cooling down.

DOI: 10.1103/PhysRevB.67.041201

PACS number(s): 61.72.-y, 66.30.-h, 78.70.Bj

The decrease of the size of the Si field-effect transistors requires extremely high doping densities in the drain and source regions. At donor concentrations above 10^{20} cm^{-3} , however, the free-electron concentration stops to increase with doping. This electrical deactivation has been attributed to the formation of compensating defects, the identification of which has been much debated.¹⁻³ Vacancy-impurity complexes have been observed in positron annihilation experiments⁴ but their exact structure is unknown. Vacancies surrounded by three As atoms, V-As₃, have been identified in Czochralski (Cz)-grown bulk Si doped up to $[\text{As}] = 10^{20} \text{ cm}^{-3}$ and their formation has been explained by kinetic migration processes.⁵⁻⁸ However, the concentration of V-As₃ complexes in Cz Si ($[\text{As}] = 10^{20} \text{ cm}^{-3}$) is only 0.1 % of the As concentration⁵ and the material does not show substantial electrical deactivation. Furthermore, it has been suggested that pairs of dopant atoms without vacancies are dominant at high doping levels.^{9,10} It is thus interesting to study the structure of compensating defect complexes at $[\text{As}] > 10^{20} \text{ cm}^{-3}$ where the electrical deactivation of doping becomes substantial. Equally important is to understand what happens to defect complexes in rapid thermal annealing (RTA) treatments which are routinely used to activate the doping after the growth.

In this paper we show that the V-As₃ complexes are the dominant vacancy defects in molecular-beam epitaxially (MBE) grown Si doped with As concentrations above 10^{20} cm^{-3} by *in situ* ion implantation during the growth. We also show that larger vacancy complexes, tentatively identified as V₂-As₅, are present at substantial concentrations. The defect complexes dissociate in annealings at 800 °C and 900 °C, respectively. Their reformation depends on the cooling time and can be explained by the elementary migration processes of vacancy-impurity complexes.⁶

We studied silicon samples with 330-nm thin MBE grown epitaxial layers doped heavily with arsenic (1.5×10^{20} and $3.5 \times 10^{20} \text{ cm}^{-3}$). The epitaxial layers were grown on *p*-type, 80 Ω cm, (001)-oriented Si float-zone refined substrates kept at a temperature of 450 °C during the growth. The growth rate was 0.02 nm/s and the As ions were im-

planted at an energy of 1 keV during the growth. The samples were subjected to annealing in N₂, either with RTA at 900 °C for 10–170 s or furnace annealing at 800°–900 °C for two minutes. Of the RTA samples, the ones annealed for 10 s were chosen for positron measurements. Before these measurements all of the samples were dipped in HF in order to remove the oxide layer which would otherwise complicate the analysis of the measurements. The electrical activities were deduced from Hall-effect/resistivity measurements on clover-leaf-shaped Van der Pauw geometries. For a couple of samples electrical activities from these integral measurements were compared to electrical activities deduced from full depth profiles measured by repeated removal of layers of 10 nm using anodic oxidation and chemical stripping. The electrical activities deduced from these two types of measurements were always found to agree within the uncertainties which are estimated to be less than 5%. The total As concentrations were determined with Rutherford backscattering spectrometry (RBS) using 2-MeV alpha particles. Both the RBS and the differential Hall/resistivity measurements demonstrated that no significant redistribution of the original As-box distribution took place during the different annealing steps.

The annealings had considerable effect on the electrical activities of the samples, as can be seen in Table I. With RTA at 900 °C the effect was strongest and found to be independent of annealing time; in Si($[\text{As}] = 1.5 \times 10^{20} \text{ cm}^{-3}$) the activity went from 20% to 98% whereas in Si($[\text{As}] = 3.5 \times 10^{20} \text{ cm}^{-3}$) it went from 2% to 85%. The annealings in the furnace at the same temperature had somewhat less of an effect, and the final activity was about 20% below the RTA value. Since the electrical activity after RTA was independent of annealing time, the lower activity after furnace annealing appears to be a result of the slower cooling-down time (~ 10 s for furnace, compared with ~ 1 s for RTA). In all cases the annealings at 800 °C had a little less of an effect on the electrical activity than corresponding annealings at 900 °C. These results show that annealing removes a large fraction of the compensating defects formed during the growth.

TABLE I. Arsenic concentrations and electrical activities of the measured samples. The concentrations of V-As₃ and V₂-As₅ defects were obtained by combining the results of electrical and positron experiments.

[As] (10 ²⁰ cm ⁻³)	Treatment	electrical activity (%)	[VAs ₃] (10 ¹⁸ cm ⁻³)	[V ₂ As ₅] (10 ¹⁸ cm ⁻³)
1.5	as grown	20	31±3	5±2
1.5	furnace at 800 °C	74	2±2	6±2
1.5	furnace at 900 °C	79	6±1	0.26±0.06
1.5	RTA at 800 °C	88		
1.5	RTA at 900 °C	98	0.4±0.2	0.38±0.08
3.5	as grown	2	80±9	20±5
3.5	furnace at 800 °C	54	1.4±0.8	24±5
3.5	furnace at 900 °C	63	28±4	9±3
3.5	RTA at 800 °C	67		
3.5	RTA at 900 °C	85	9±2	5±2

In the positron annihilation experiments, we measured the Doppler broadening of the annihilation radiation using Ge detectors. The coincidence detection of both 511-keV photons emitted from the $e^+ - e^-$ annihilation was accomplished by a two-parameter multichannel analyzer. This experiment allows identification of vacancies by recording the momentum distribution of annihilating electrons. An energy resolution of 1.0 keV and a peak-to-background ratio of 2×10^6 were achieved in the coincidence mode. From the Doppler spectra we calculated the shape parameters S and W . S describes annihilations with the valence electrons and W with the outermost core electrons.

The measured W parameters (measured with one Ge detector) in as-grown and RTA treated Si([As]= 1.5×10^{20} cm⁻³) samples are shown in Fig. 1 as a function of positron implantation energy E . The W (and S) parameters are constant at $E=1-4$ keV in all the samples except in the RTA treated Si([As]= 1.5×10^{20} cm⁻³). With increasing E the W parameter decreases to the level obtained in the defect-free Si lattice in the substrate. The 330-nm highly doped Si layer can thus be characterized with the large W parameter at $E=1-4$ keV.

The constant W and S parameters at $E=1-4$ keV show that positrons stopped at the heavily doped layer do not diffuse efficiently but annihilate in the layer. In fact, if we assume no positron diffusion after thermalization, we can reproduce the experimental $W(E)$ curve in the as-grown Si([As]= 1.5×10^{20} cm⁻³) sample as shown in Fig. 1. This means that due to strong positron trapping at vacancies the positron diffusion length is $\leq 10\%$ of the thickness of the As-doped layer (330 nm). The associated positron trapping rate is $\kappa \sim (220 \text{ nm}/30 \text{ nm})^2 \lambda_b \sim 500 \text{ ns}^{-1}$ (the positron annihilation rate is $\lambda_b \sim 5 \text{ ns}^{-1}$ and diffusion length is ~ 220 nm in defect-free Si). Using the trapping coefficient of $\mu = 10^{15} \text{ s}^{-1}$ the vacancy concentration in the As-doped Si layer is thus $> 10^{19} \text{ cm}^{-3}$. Only in the RTA treated Si([As]= 1.5×10^{20} cm⁻³) sample (Fig. 1) is the positron diffusion obviously stronger and the vacancy concentration an order-of-magnitude lower.

The core electron momentum distributions at the vacancies were measured by implanting 3-keV positrons to the

highly As-doped layer (Fig. 2). The intensity of the spectra is well above that recorded in defect-free Si. This effect is the opposite from that expected for clean vacancies, but a direct indication of As atoms in the surroundings of vacancies.⁵ The ten $3d$ core electrons of As atoms increase the core electron density and positron annihilation probability with them. The data of Fig. 2 are very similar to that recorded earlier for a vacancy surrounded by three As atoms, the V-As₃ complex.⁵

Our measurements thus show that V-As₃ complexes exist in high concentrations (above 10^{19} cm^{-3}) in MBE-grown

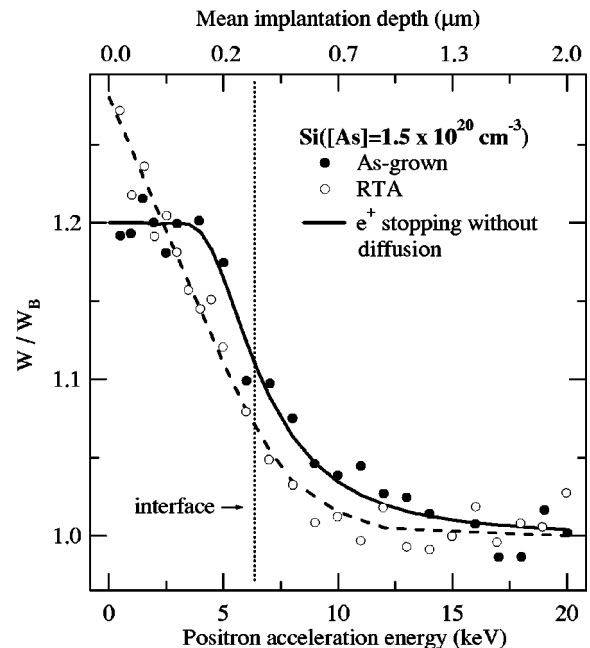


FIG. 1. W parameter (10^{-16}) $\times 10^{-3} m_0 c$ as a function of positron incident energy. The data is shown as scaled to the W parameter measured in the defect-free Si lattice. The incident positron energy is converted to the mean positron stopping depth in the top axis. The solid line shows the $W(E)$ curve calculated assuming no positron diffusion after stopping. The dashed line is to guide the eye and the dotted vertical line shows the boundary of the highly As-doped layer at 330 nm.

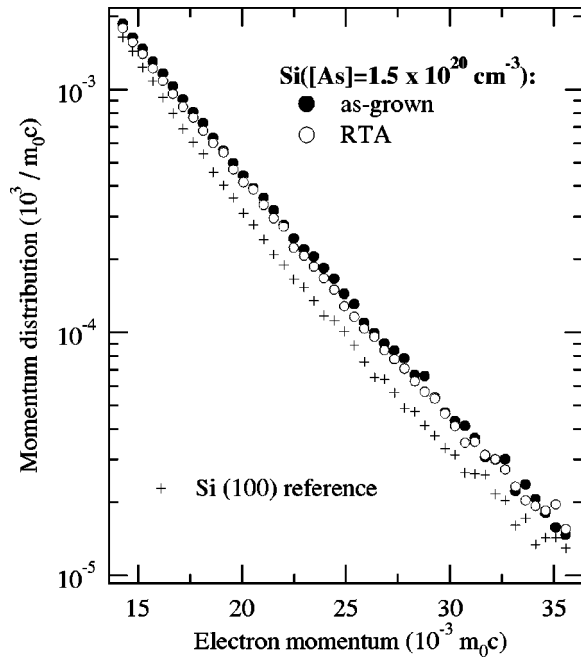


FIG. 2. Core electron momentum distributions measured in the sample $\text{Si}([\text{As}] = 1.5 \times 10^{20} \text{ cm}^{-3})$ and in the defect-free reference sample.

silicon doped to very high doping levels by *in situ* ion implantation. Previously these V-As_3 defects have been identified in Czochralski-grown $\text{Si}([\text{As}] = 10^{20} \text{ cm}^{-3})$, but at a considerably lower concentration (10^{17} cm^{-3}).⁵ The high concentration of these defects in as-grown samples gives strong evidence that they are responsible for the electrical deactivation observed in silicon with very high doping.

However, the details of the Doppler broadening data show that larger V-As complexes are also present. The linearity of valence and core electron momentum distributions is studied in Fig. 3, which shows the W parameters in all samples as a function of the S parameter. The measurements were made using a coincidence of two Ge detectors allowing us to record the W parameter at higher momentum values ($20\text{--}25 \times 10^{-3} m_0c$) and the deconvolution of the energy resolution for the S parameter. All points except that measured in the RTA treated $\text{Si}([\text{As}] = 1.5 \times 10^{20} \text{ cm}^{-3})$ fall on a line where the W parameter is almost constant but S varies. The line crosses the (S, W) point corresponding to the V-As_3 defect (obtained in Ref. 5) but does not approach the (S, W) point of the defect-free Si lattice along the dashed line in Fig. 3. This indicates that another vacancy complex coexists with V-As_3 in the highly As-doped material. Its characteristic S parameter is larger than that of V-As_3 indicating that the open volume is larger. Since the W parameter is about the same as that for V-As_3 , the relative number of As surrounding the defect is the same. The simplest of such defects at the right side of the SW plot are the $\text{V}_2\text{-As}_n$ complexes, with $n = 4, 5$. A quantitative calculation (using methods described in Ref. 11) shows that the most likely assignment of the defect is $\text{V}_2\text{-As}_5$. Notice that in the samples with the higher As concentration the W parameters in Fig. 3 are systematically larger. This may indicate that the average number of As sur-

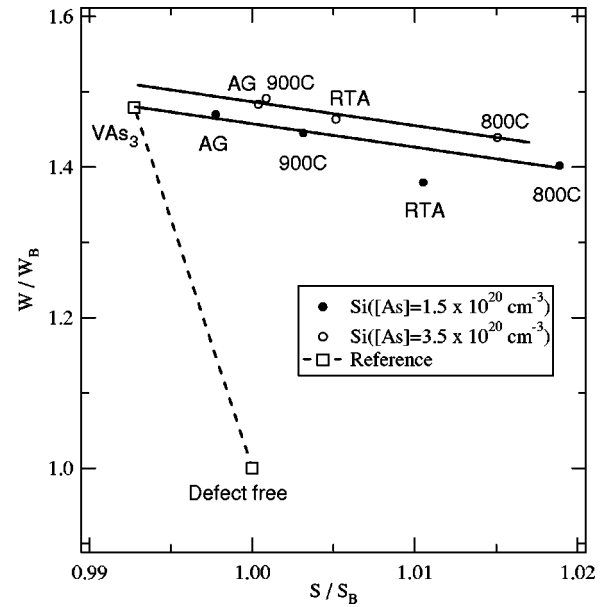


FIG. 3. Relative W parameters ($20\text{--}25 \times 10^{-3} m_0c$) as a function of relative S parameters ($0\text{--}3 \times 10^{-3} m_0c$) from all the measured samples and a sample containing V-As_3 defects. All measurements were done using a coincidence setup of two Ge detectors. The energy resolution function was deconvoluted out of the spectrum before the calculation of the S parameter. AG in the plot denotes as-grown samples.

rounding vacancies is slightly larger, e.g., due to the formation of small concentrations of V-As_4 .

The positron diffusion lengths (Fig. 1) are able to yield the order of magnitudes of vacancy complex concentrations, which are $> 10^{19} \text{ cm}^{-3}$ in as grown and $10^{17}\text{--}10^{19} \text{ cm}^{-3}$ in the annealed samples. These concentrations are high enough to explain the electrical deactivation. We thus conclude that other defects, such as As clusters without a vacancy, contribute less to the compensation. To estimate the vacancy concentrations more accurately and compare them after various annealings we combine the positron results with the electrical data. We assume that all positrons annihilate at the two dominant defects, V-As_3 and $\text{V}_2\text{-As}_5$, and that these defects are the only ones participating in the compensation. We take the S parameter of $1.02\text{--}1.04$ for $\text{V}_2\text{-As}_5$ on the basis of (i) experimental data for V-As_n and $\text{V}_2\text{-As}_n$,^{5,6,12} (ii) calculated results for V-As_n and $\text{V}_2\text{-As}_n$,⁵ and (iii) the lower limit of 1.02 set by the data of Fig. 3. The fraction f_{pass} of electrically inactive As and the S parameter in Fig. 3 can now be written as

$$f_{pass}[\text{As}] = 3[\text{VAs}_3] + 5[\text{V}_2\text{As}_5], \quad (1)$$

$$S = \frac{[\text{VAs}_3]S(\text{VAs}_3) + [\text{V}_2\text{As}_5]S(\text{V}_2\text{As}_5)}{[\text{VAs}_3] + [\text{V}_2\text{As}_5]}, \quad (2)$$

where we have assumed that the positron trapping coefficients at both vacancy complexes are the same. The estimated defect concentrations, obtained by solving Eqs. (1) and (2), are shown in Table I. The error limits are mainly due to the uncertainties of the S parameter of the $\text{V}_2\text{-As}_5$ defect.

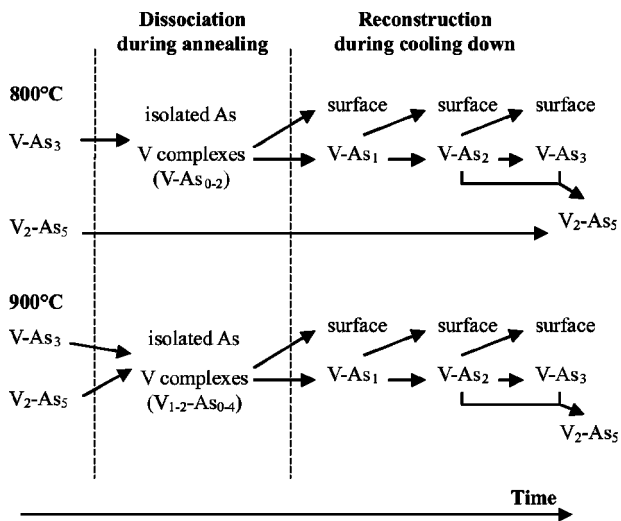


FIG. 4. Effect of annealing in highly doped Si. The dissociation of $V\text{-As}_3$ and $V_2\text{-As}_5$ leave behind electrically active isolated As and vacancy complexes such as V, V-As, and V-As₂. During cooling down these complexes migrate and passivate As impurities by binding them to larger vacancy complexes. The elementary chain reaction starting from an isolated vacancy is shown in the figure.

The defect concentrations in Table I indicate that the dominant defect in as-grown samples is $V\text{-As}_3$. With annealing the relative amount of $V_2\text{-As}_5$ increases, and even dominates after annealing at 800 °C. Obviously the $V\text{-As}_3$ and $V_2\text{-As}_5$ complexes become unstable at 800 °C and 900 °C, respectively, since their concentrations decrease. The rapid thermal annealing leaves behind less vacancy complexes than the longer annealing in the furnace at the same temperature demonstrating the importance of the cooling time in the reconstruction of the deactivating defects.

In Fig. 4 we propose defect reactions taking place in highly As-doped Si in the annealing and cooling down. At 800 °C the $V\text{-As}_3$ defects disintegrate and leave behind V, V-As, and V-As₂ defects, which are mobile.⁶ These complexes continue diffusing during the cooling down, and may

pair with As to finally reconstruct $V\text{-As}_3$. The heat treatments cause a significant decrease in the total vacancy concentration which indicates that migrating vacancy complexes have a chance to reach the surface where the vacancy can escape. The $V_2\text{-As}_5$ complexes present before the annealing remain in the sample, and their concentrations can also increase when, for example, $V\text{-As}_2$ and $V\text{-As}_3$ combine.

In annealings at 900 °C also the $V_2\text{-As}_5$ defects break up, whereafter the processes continue as after 800 °C annealing. However, at higher temperatures the defects are more mobile and more vacancies thus have a chance to escape the sample or form defects. Interestingly the $V\text{-As}_3$ concentration is larger after 900 °C than after 800 °C annealing. This behavior, however, is consistent with the kinetic model of Fig. 4. The $V_2\text{-As}_5$ defects dissociating at 900 °C are additional sources for migrating V, V-As, and V-As₂, which form stable $V\text{-As}_3$ complexes during the cooling down at $T < 800$ °C.

In RTA both the heat treatment and the cooling take place more rapidly than in furnace annealing. In general the migrating species have thus less time to form the $V\text{-As}_3$ and $V_2\text{-As}_5$ defects during the cooling down. This explains the higher electrical activity of As after rapid thermal annealing as observed here and in Ref. 13 earlier. However, notice that in addition to the processes of Fig. 4 also some $V\text{-As}_4$ and other vacancy complexes may form but their concentrations are much lower.

In conclusion, we have shown that a vacancy surrounded by three As atoms is the dominant compensating vacancy defect in heavily As-doped MBE-grown Si. Larger vacancy complexes, tentatively identified as $V_2\text{-As}_5$, are also formed at high concentrations. The $V\text{-As}_3$ and $V_2\text{-As}_5$ complexes are removed by annealings at 800 °C and 900 °C, respectively. However, they are likely to reconstruct during the cooling down by subsequent migrations of V, V-As, and V-As₂. The rapid thermal annealing is shown to lead to smallest concentrations of $V\text{-As}_3$ and $V_2\text{-As}_5$ complexes, most likely due to the limited time available for the migration processes.

¹P.A. Packan, Science **285**, 2079 (1999).

²A. Nylandsted Larsen, K.K. Larsen, and P.E. Andersen, J. Appl. Phys. **73**, 691 (1993).

³P.M. Fahey, P. Griffin, and J.D. Plummer, Rev. Mod. Phys. **61**, 289 (1989).

⁴D.W. Lawther, U. Myler, P.J. Simpson, P.M. Rousseau, P.B. Griffin, and J.D. Plummer, Appl. Phys. Lett. **67**, 3575 (1995).

⁵K. Saarinen, J. Nissilä, H. Kauppinen, M. Hakala, M.J. Puska, P. Hautojärvi, and C. Corbel, Phys. Rev. Lett. **82**, 1883 (1999).

⁶V. Ranki, J. Nissilä, and K. Saarinen, Phys. Rev. Lett. **88**, 105506 (2002).

⁷J. Xie and S.P. Chen, Phys. Rev. Lett. **83**, 1795 (1999).

⁸M. Ramamoorthy and S.T. Pantelides, Phys. Rev. Lett. **76**, 4753 (1996).

⁹D.J. Chadi, P.H. Citrin, C.H. Park, D.L. Adler, M.A. Marcus, and H.-J. Gossmann, Phys. Rev. Lett. **79**, 4834 (1997).

¹⁰P.M. Voyles, D.A. Muller, J.L. Grazul, P.H. Citrin, and H.-J.L. Gossmann, Nature (London) **416**, 826 (2002).

¹¹M. Alatalo, B. Barbiellini, M. Hakala, H. Kauppinen, T. Korhonen, M.J. Puska, K. Saarinen, P. Hautojärvi, and R.M. Nieminen, Phys. Rev. B **54**, 2397 (1996).

¹²H. Kauppinen, C. Corbel, J. Nissilä, K. Saarinen, and P. Hautojärvi, Phys. Rev. B **57**, 12911 (1998).

¹³A. Nylandsted Larsen, B. Christensen, and S.Yu. Shiryayev, J. Appl. Phys. **71**, 4854 (1992).